

**How Additives for Tin Halide Perovskites Influence the Sn<sup>4+</sup> Concentration**

Journal:	<i>Journal of Materials Chemistry A</i>
Manuscript ID	TA-ART-02-2022-001429.R1
Article Type:	Paper
Date Submitted by the Author:	20-May-2022
Complete List of Authors:	Joy, Syed; University of Kentucky, Chemistry Atapattu, Harindi; University of Kentucky, Department of Chemistry Sorensen, Stephanie; University of Kentucky, Chemistry Pruett, Henry; University of Kentucky, Chemistry Olivelli, Alexander; University of Kentucky, Chemistry Huckaba, Aron; University of Kentucky, Department of Chemistry Miller, Anne-Frances; University of Kentucky, Chemistry Graham, Kenneth; University of Kentucky, Chemistry

## How Additives for Tin Halide Perovskites Influence the Sn<sup>4+</sup> Concentration

Syed Joy, Harindi R. Atapattu, Stephanie Sorensen, Henry Pruet, Alexander B. Olivelli, Aron J. Huckaba, Anne-Frances Miller, and Kenneth R. Graham\*

Department of Chemistry, University of Kentucky, Lexington, Kentucky 40506, USA

\*E-mail: [Kenneth.graham@uky.edu](mailto:Kenneth.graham@uky.edu)

### Abstract:

Tin halide perovskite (Sn-HPs) photovoltaics could potentially equal or exceed the performance of their more toxic Pb-based analogues if defect state densities, particularly originating from the presence of Sn<sup>4+</sup>, can be significantly decreased. Numerous additives are incorporated into Sn-HPs to minimize the amount of Sn<sup>4+</sup>, including SnF<sub>2</sub>, reducing agents such as hydrazine derivatives, and various antioxidants. Despite the frequent use of additives to reduce Sn<sup>4+</sup> content, there is limited understanding of how they function and consequently limited guidance for the development of new additives. Herein, we use cyclic voltammetry to probe the redox behavior of SnI<sub>2</sub>, SnI<sub>4</sub>, Sn-HP precursor solutions, and 18 different additives. Through <sup>119</sup>Sn NMR measurements we show that hydrochloride containing additives undergo halide exchange with SnI<sub>4</sub> to form SnI<sub>x</sub>Cl<sub>y</sub>, which results in decreased Sn<sup>4+</sup> concentrations and less p-type character in the Sn-HP films. We find that the most effective additive at lowering the Sn<sup>4+</sup> content in FASnI<sub>3</sub> is not capable of reducing SnI<sub>4</sub> or forming SnI<sub>x</sub>Cl<sub>y</sub>, but rather it acts as a sacrificial and coordinating antioxidant. In general, when selecting additives for Sn-HPs it is important to account for the redox potential, coordination with Sn species, ability to react with oxygen, and the potential for halide exchange.

**Introduction:**

Organic metal halide perovskite (HP) based solar cells (PSCs) are widely considered as the most promising materials for high efficiency and low-cost photovoltaics (PVs), with the power conversion efficiency (PCE) of Pb-based PSCs increasing from 3.8 to 25.2% within just over a decade of intensive research efforts.<sup>1,2</sup> Nevertheless, these Pb-based PSCs face several impediments to widespread commercialization, one of which is the toxicity of Pb. Desire for less-toxic PSCs has motivated intense efforts to identify Pb-free HPs for PSCs, with Sn-HPs currently being the front-runners.<sup>3-6</sup> Tin has a similar ionic radius (118 pm and 119 pm for Sn<sup>2+</sup> and Pb<sup>2+</sup>, respectively),<sup>7</sup> relatively high charge-carrier mobilities,<sup>8,9</sup> and a near-ideal bandgap (~1.3 eV) for reaching high PCEs.<sup>6,10</sup> However, the highest certified PCE for Sn-based PSCs to date is 14.6%,<sup>4</sup> which is much lower than the Pb analogues. Current understanding is that the biggest impediment to high Sn-PSC performance is the oxidation of Sn<sup>2+</sup> to Sn<sup>4+</sup>,<sup>3,6,11</sup> which results in deformation of the perovskite structure, defect state introduction, and rapid degradation of device performance. Thus, a major challenge for Sn-PSC development is to minimize Sn<sup>4+</sup> content.

Oxidation of Sn-HPs can lead to SnI<sub>4</sub> formation and eventually I<sub>2</sub> as degradation products, which perpetuates an oxidative degradation cycle that continuously deteriorates the material and device.<sup>12</sup> Furthermore, SnI<sub>4</sub> is present as an impurity in the SnI<sub>2</sub> precursors used to form Sn-HPs.<sup>13</sup> Eliminating or minimizing Sn<sup>4+</sup> is critical and central to all reports of relatively high-performing Sn-PSCs. Strategies to eliminate Sn<sup>4+</sup> include purifying SnI<sub>2</sub> or synthesizing high purity SnI<sub>2</sub> to minimize SnI<sub>4</sub> content in the precursor,<sup>4,13</sup> using reducing agents to reduce Sn<sup>4+</sup> impurities to Sn<sup>2+</sup>,<sup>14</sup> using antioxidants to prevent the formation of Sn<sup>4+</sup>,<sup>15,16</sup> and adding bulky A-site cations to

stabilize the resulting films.<sup>17,18</sup> A combination of these strategies is often used to fabricate high-performing Sn-PSCs.<sup>4,19</sup>

Various additives have been explored to limit the amount of Sn<sup>4+</sup> present in HPs, with the proposed mechanism based on either Sn<sup>4+</sup> to Sn<sup>2+</sup> reduction or retarding the oxidation of Sn<sup>2+</sup>.<sup>14–16,20,21</sup> These additives include SnF<sub>2</sub> and SnCl<sub>2</sub>,<sup>22–24</sup> hydrazine and hydrazine containing compounds,<sup>14,21,25–29</sup> metallic tin,<sup>30</sup> and organic acids.<sup>15,16,20</sup> Although these additives are highly important, the mechanisms of action often remain unclear. For example, the mechanistic understanding for even the most common additive for Sn-HPs, SnF<sub>2</sub>, continues to evolve.<sup>24,31,32</sup> Previously, SnF<sub>2</sub> was often regarded as a reducing additive; however, a detailed investigation by Pascual *et. al.*<sup>32</sup> showed that SnF<sub>2</sub> does not reduce Sn<sup>4+</sup> but instead undergoes a ligand exchange with SnI<sub>4</sub> to form SnI<sub>2</sub> and SnF<sub>4</sub>. Here, the authors attribute the improved PSC performance with SnF<sub>2</sub> addition to the exclusion of Sn<sup>4+</sup> from the FASnI<sub>3</sub> crystalline grains.

In an early investigation, Song *et. al.*<sup>21</sup> reported that hydrazine (N<sub>2</sub>H<sub>4</sub>) vapor creates a reducing environment to suppress the formation of Sn<sup>4+</sup> during tin perovskite deposition. Following this report, several groups used hydrazinium iodide and hydrazine dihydrochloride to reduce the amount of Sn<sup>4+</sup> and further improve the PCE and stability of Sn PSCs.<sup>25–28</sup> These reports suggest that hydrazine and its HI and HCl salts could reduce Sn<sup>4+</sup>; however, no direct proof was offered to show that Sn<sup>4+</sup> reduction occurs. Importantly, the reduction and oxidation potentials of both the Sn species (e.g., SnI<sub>2</sub> and SnI<sub>4</sub>) and the hydrazine derivatives may depend on the solvent, solution pH, and reactants present.<sup>20,33</sup> Consequently, standard redox potentials reported in aqueous solutions may lead to incorrect predictions regarding redox activity in anhydrous organic solvents.

Metallic Sn, if appropriately removed from the precursor solution prior to HP film formation, can serve as an effective reducing agent for  $\text{Sn}^{4+}$  to yield improved PSCs.<sup>30,34</sup> Here, metallic Sn undergoes a comproportionation reaction with  $\text{Sn}^{4+}$  to form  $\text{Sn}^{2+}$ .<sup>30</sup> Various acids have also been investigated as reducing agents and antioxidants, including hypophosphorous acid,<sup>35</sup> formic acid,<sup>36</sup> hydroquinonesulfonic acid potassium salt,<sup>15</sup> ascorbic acid,<sup>37</sup> and caffeic acid.<sup>16</sup> These examples of organic acids appear to involve the additive acting as an antioxidant rather than a reducing agent. However, whether the additive acts as an antioxidant or reducing agent is ambiguous in many reports.

Despite the significant amount of investigation into decreasing the amount of  $\text{Sn}^{4+}$  in films, there is a dearth of mechanistic understanding on how different additives function and what aspects are most important. Additives may decrease the  $\text{Sn}^{4+}$  concentration via three primary mechanisms, which include acting as reducing agents to directly convert  $\text{Sn}^{4+}$  to  $\text{Sn}^{2+}$ , preventing  $\text{Sn}^{2+}$  oxidation, or reacting with  $\text{Sn}^{4+}$  to make it more benign, as observed for  $\text{SnF}_2$  addition. In the case of antioxidants, these may react with  $\text{O}_2$  to prevent  $\text{O}_2$  from oxidizing the Sn-HP or they may coordinate  $\text{Sn}^{2+}$  at the film surface or at grain boundaries to make the Sn-HP less susceptible to oxidation.<sup>15,20,38</sup> Occasionally, antioxidant and reducing agent are used interchangeably in the literature, yet antioxidants are often incapable of acting as reducing agents for the species of interest. For instance, an antioxidant may react with oxidizing agents to prevent them from oxidizing the compound of interest or coordinate the compound of interest to reduce its susceptibility to oxidation.

The work presented herein seeks to improve our mechanistic understanding of how various additives diminish the amount of  $\text{Sn}^{4+}$  in thin films. Included in this investigation are additives that may reduce  $\text{Sn}^{4+}$ , coordinate  $\text{Sn}^{2+}$  in solution without reducing  $\text{Sn}^{4+}$ , act as sacrificial antioxidants,

or facilitate a halide exchange with  $\text{SnI}_4$ . First, we use electrochemistry to probe redox activity of the HP precursors in the typically used DMF:DMSO processing solution, including  $\text{SnI}_2$  and  $\text{SnI}_4$ , as well as the redox potentials of a host of additives. This electrochemistry data provides a first assessment of the thermodynamic favorability of  $\text{SnI}_4$  reduction. Using a combination of CV,  $^1\text{H}$  and  $^{119}\text{Sn}$  NMR, x-ray photoemission spectroscopy (XPS), and ultraviolet photoemission spectroscopy (UPS), we determine the impact of additives on the concentration of  $\text{Sn}^{4+}$  in solution and in thin films.

### Results and Discussion:

Cyclic voltammetry (CV) provides a direct way to measure reduction and oxidation of Sn-HP precursors in solution. Herein, we focus our discussion on anodic ( $E_{p,a}$ ) and cathodic ( $E_{p,c}$ ) peak potentials, as the reduction potentials for some species cannot be determined due to the irreversibility of the electrochemical reaction. To ensure that the anodic and cathodic potentials reported are directly relevant to Sn-HPs, we measured CVs in both pure DMF and the commonly used DMF:DMSO (4:1) solvent system. Although DMSO can act as an oxidizing agent for  $\text{SnI}_2$ ,<sup>39,40</sup> the CV spectra for the formamidinium tin iodide ( $\text{FASnI}_3$ ) precursors in DMF and DMF:DMSO solutions are nearly identical, as shown in Figure 1 and SI Figure S1. Tin (II) iodide shows a  $E_{p,c}$  of -1.15 V (vs.  $\text{Ag}/\text{Ag}^+$ ), whereas  $E_{p,c}$  for  $\text{SnI}_4$  occurs at -0.72 V. Films of  $\text{FASnI}_3$  also show nearly the same onset for the cathodic wave of  $\text{Sn}^{2+}$  as is observed for  $\text{SnI}_2$  in solution, with an  $E_{p,c}$  of -1.20 V (vs.  $\text{Ag}/\text{Ag}^+$ ) (Figure S2). The  $E_{1/2}$  for  $\text{SnI}_2 + 2e^- \leftrightarrow \text{Sn}^0 + 2\text{I}^-$  is -1.02 V; however, with an irreversible reduction the  $E_{1/2}$  for  $\text{SnI}_4 + 2e^- \leftrightarrow \text{SnI}_2 + 2\text{I}^-$  cannot be determined. The commonly used additive  $\text{SnF}_2$  shows a more negative  $E_{1/2}$  than  $\text{SnI}_2$  at -1.13 V. Given the reduction behavior of  $\text{SnI}_2$  and  $\text{SnI}_4$ , ideal reducing agents for reducing  $\text{SnI}_4$  to  $\text{SnI}_2$  should have redox potentials in the range of *ca.* -0.75 to -1.0 V vs.  $\text{Ag}/\text{Ag}^+$  when measured in DMF:DMSO. In this

range  $\text{SnI}_4$  reduction to  $\text{SnI}_2$  is thermodynamically favorable, while further reduction to metallic Sn is not favorable. That is, the upper limit of this recommend range (*ca.* -0.75 V) is more negative than the  $E_{p,c}$  for  $\text{SnI}_4$  (-0.72 V) and thus reduction of  $\text{SnI}_4$  to  $\text{SnI}_2$  is favorable, while the lower limit (*ca.* -1.0 V) avoids reducing  $\text{SnI}_2$  to metallic Sn, as  $\text{SnI}_2$  shows an onset of reduction at *ca.* -1.04.

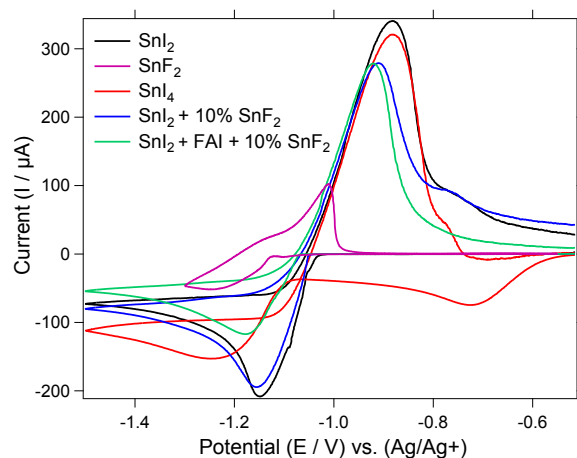


**Figure 1.** CV of  $\text{SnI}_2$ ,  $\text{SnF}_2$ ,  $\text{SnI}_4$ ,  $\text{SnI}_2 + 10\% \text{SnF}_2$ , and  $\text{SnI}_2 + \text{FAI} + 10\% \text{SnF}_2$  in DMF:DMSO (4:1) with 0.1 M TBAPF<sub>6</sub> as the supporting electrolyte.

With the oxidation and reduction behavior of  $\text{SnI}_2$  and  $\text{SnI}_4$  in DMSO:DMF determined, we now turn to investigating the influence of the additives. To investigate the mechanism through which several reported additives for Sn HPs function and to identify new additives, the molecules and complexes shown in Figure 2a were initially investigated with CV, as shown in Figure 2b and c. The additives investigated include quinones and hydroxyquinones, catechols and structurally related derivatives, hydrazine containing derivatives, and hydrochloride containing species. Specifically, the quinones and hydroxyquinones are selected for their large variation in redox potentials, the catechols for their anticipated abilities to coordinate Sn halides, and the hydrazine derivatives for their low oxidation potentials that make them amenable for use as reducing agents.

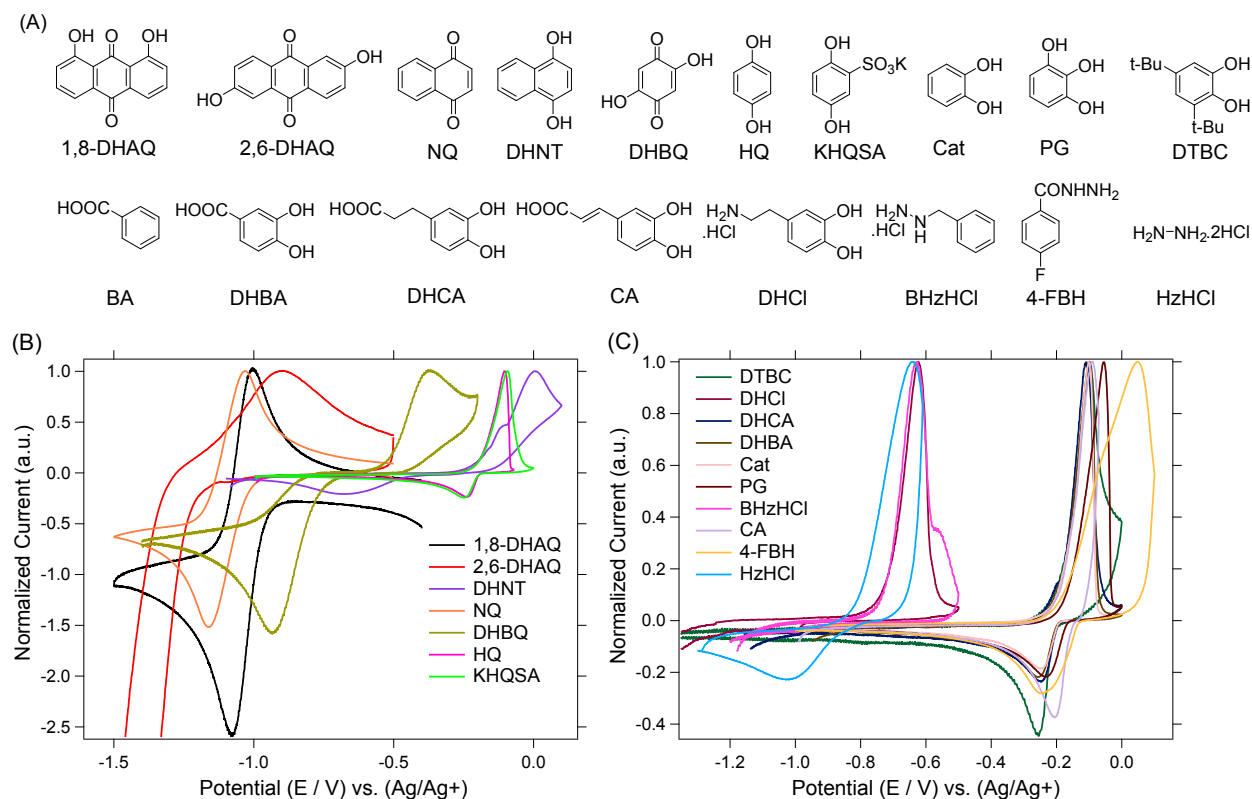


**Figure 2.** Chemical structures (A) and CV of additives (B and C) in DMF:DMSO (4:1) with 0.1 M TBAPF<sub>6</sub> as the supporting electrolyte.

The CV data show three clusters of anodic peaks, with the dihydroxyanthroquinone derivatives (1,8-DHAQ and 2,6-DHAQ) and naphthoquinone (NQ) showing  $E_{p,a}$  near -1.0 V; the hydrochloride (HCl) salts including dopamine HCl (DHCl), benzylhydrazine HCl (BzHCl), and hydrazine HCl (HzHCl) showing  $E_{p,a}$  near -0.6 V; and the catechol and hydroquinone derivatives displaying  $E_{p,a}$  close to -0.1 V. One additive, 2,5-dihydroxy-1,4-benzoquinone (DHBQ), has  $E_{p,a}$  outside of these regions at -0.37 V. Based on these anodic peak positions and  $E_{1/2}$  values, HzHCl, BzHCl, and DHCl are near the range where SnI<sub>4</sub> to SnI<sub>2</sub> reduction becomes favorable, while 1,8-DHAQ, 2,6-DHAQ, and NQ are in a range where SnI<sub>4</sub> to SnI<sub>2</sub> reduction is favorable with the possibility of SnI<sub>2</sub> to metallic Sn reduction occurring. However, to act as reducing agents the additives must originally be in their reduced form, which is not the case with 1,8-DHAQ, 2,6-

DHAQ, and NQ. A commercially available reduced form of NQ, DHNT, shows an anodic peak near 0 V and an  $E_{1/2}$  of -0.33 V, which is not appropriate for reducing  $\text{SnI}_4$ . The fact that the electrochemically reduced form of NQ does not show an anodic peak at the same potential as DHNT indicates that NQ does not undergo a two-proton coupled electron transfer upon reduction in the DMF:DMSO solvent system, as it does in aqueous solution.<sup>41</sup> Rather, the electrochemically reduced form of NQ is a singly charged anion.<sup>41</sup>

**Table 1:** Anodic and cathodic peak potentials of  $\text{SnI}_2$ ,  $\text{SnI}_4$ , and additives.  $E_{p,a}$ ,  $E_{p,c}$  and  $E_{1/2}$  values are reported vs.  $\text{Ag}/\text{Ag}^+$  (1 M) reference electrode.

Compound	$E_{p,a}$ (V)	$E_{p,c}$ (V)	$E_{1/2}$ (V)
$\text{SnI}_2$ ( $\text{SnI}_2 \leftrightarrow \text{Sn}^0$ )	-0.88	-1.15	-1.02
$\text{SnI}_4$ ( $\text{SnI}_4 \leftrightarrow \text{SnI}_2$ )	NA*	-0.72	NA
$\text{SnF}_2$ ( $\text{SnF}_2 \leftrightarrow \text{Sn}^0$ )	-1.01	-1.25	-1.13
Cat	-0.10	-0.25	-0.18
PG	-0.05	-0.23	-0.14
DTBC	-0.09	-0.26	-0.18
DHBA	-0.10	-0.25	-0.18
CA	-0.09	-0.21	-0.15
DHCA	-0.10	-0.24	-0.17
DHCl	-0.65	NA	NA
BHzHCl	-0.63	NA	NA
HQ	-0.10	-0.24	-0.17
KHQSA	-0.09	-0.25	-0.17
4-FBH	0.05	-0.25	-0.10
HzHCl	-0.64	-1.03	-0.84
DHBQ	-0.37	-0.93	-0.65**
NQ	-1.03	-1.16	-1.09
DHNT	0.008	-0.67	-0.33**
1,8-DHAQ	-0.99	-1.12	-1.06
2,6-DHAQ	-0.93	-1.45	-1.19**

\*NA indicates that peak was not observed. If either the cathodic or anodic peak is missing, then  $E_{1/2}$  cannot be calculated. \*\*Quasireversible process,  $E_{1/2}$  calculated from the anodic and cathodic peak potential.

Several additives that were shown to decrease the amount of  $\text{Sn}^{4+}$  present in Sn-HPs, including caffeic acid (CA),<sup>16</sup> potassium hydroquinonesulfonate (KHQSA),<sup>15</sup> and 4-fluorobenzohydrazide (4-FBH),<sup>38</sup> show  $E_{p,a}$  and  $E_{1/2}$  values that are far too positive to act as reducing agents for  $\text{SnI}_4$ . The fact that all three of these additives have been shown to diminish the concentration of  $\text{Sn}^{4+}$  in Sn-HPs indicates that something other than  $\text{SnI}_4$  reduction is occurring, likely involving coordination to  $\text{Sn}^{2+}$  to prevent oxidation. Another additive that was demonstrated to decrease the  $\text{Sn}^{4+}$  concentration, HzHCl, has an  $E_{p,a}$  of -0.64 V and an  $E_{1/2}$  in the ideal range for  $\text{SnI}_4$  reduction without over reduction to metallic Sn at -0.84 V. Additionally, BHzHCl and DHCl show similar anodic peaks of -0.63 and -0.65 V, respectively, suggesting that they may also be able to reduce  $\text{SnI}_4$  to some extent. To further probe the ability of selected additives to reduce  $\text{SnI}_4$  we carried out solution state  $^{119}\text{Sn}$  NMR measurements.

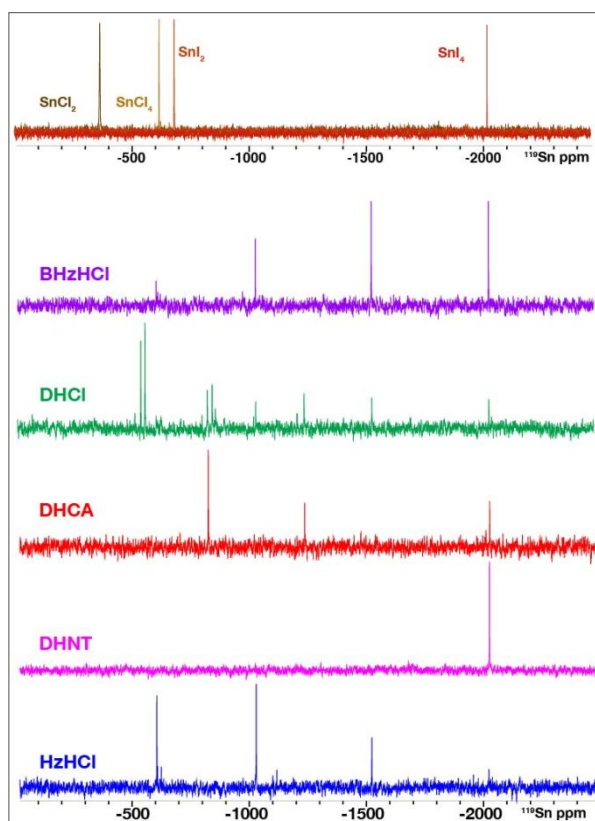


**Figure 3.**  $^{119}\text{Sn}$  NMR of the reference Sn compounds ( $\text{SnI}_2$ ,  $\text{SnI}_4$ ,  $\text{SnCl}_2$ ,  $\text{SnCl}_4$ ) (top) and  $\text{SnI}_4$  + additive (1:1 mole ratio) in  $\text{DMSO}-d_6$ .

The  $^{119}\text{Sn}$  NMR shows clear and well separated peaks for  $\text{SnI}_2$  and  $\text{SnI}_4$ . Here,  $\text{SnI}_4$  shows a signal at a chemical shift of -2025 ppm while  $\text{SnI}_2$  falls at -691 ppm. To probe for  $\text{SnI}_4$  to  $\text{SnI}_2$  reduction, selected additives were added to  $\text{SnI}_4$  in DMSO solutions at a 1:1 concentration and  $^{119}\text{Sn}$  NMR spectra recorded, as shown in Figure 3 and S10. No clear evidence of  $\text{SnI}_4$  reduction to  $\text{SnI}_2$  is observed for any of the additives investigated; although, it cannot be excluded that some of the peaks in the -500 to -700 ppm range correspond with complexes of  $\text{SnI}_2$ . The three additives with  $E_{p,a}$  in the -0.63 to -0.65 V range all show the presence of several other Sn peaks; however, none of these peaks align directly with  $\text{SnI}_2$ . Notably, all these additives (BHzHCl, DHCl, and HzHCl) contain HCl. All three display peaks at -606 ppm near that of  $\text{SnCl}_4$ , as well as peaks at *ca.* -1030 and -1525 ppm, which we attribute to the presence of  $\text{SnI}_2\text{Cl}_2$  and  $\text{SnI}_3\text{Cl}$ , respectively.<sup>42,43</sup> These products originate from halide exchange, similar to that observed between  $\text{SnI}_4$  and  $\text{SnF}_2$ .<sup>32</sup> This halide exchange does not depend on the oxidation potential of the additives, as it also occurs when methylammonium chloride is added to  $\text{SnI}_4$ , as shown in SI Figures S10 and S11. A series of  $^{119}\text{Sn}$  NMR and UV-Vis absorbance spectra were recorded with varying  $\text{SnI}_4$ :MACl ratios to further support the NMR peak assignments and the formation of  $\text{SnI}_x\text{Cl}_y$  species, as shown in SI Figure S11. Here, the  $^{119}\text{Sn}$  NMR shows that as the ratio of  $\text{SnI}_4$ :MACl decreases the peak intensities corresponding with increased y values in  $\text{SnI}_x\text{Cl}_y$  increase, while the UV-Vis shows a decrease in  $\text{SnI}_4$  absorbance intensity and a blue shift in absorbance maxima as the amount of MACl increases. At a 1:4 ratio, where the moles of I and Cl are equal, Cl completely displaces I and results in the presence of only  $\text{SnCl}_4$  in the  $^{119}\text{Sn}$  NMR spectra. In accordance with the explanation for F exchange with I in  $\text{SnI}_4$ ,<sup>32</sup> the Cl exchange can also be attributed to the

increased stability of  $\text{SnCl}_4$  relative to  $\text{SnI}_4$  described by hard-soft acid-base theory. The formation of  $\text{SnI}_x\text{Cl}_y$  complexes is likely to have a significant influence on the resulting defect states in Sn-HPs, potentially leading to exclusion of the  $\text{Sn}^{4+}$  species from the  $\text{FASnI}_3$  crystalline grains or a change in the energies of the resulting defect states. Additionally, these species may evaporate from the film considering the relatively low boiling point of  $\text{SnCl}_4$  of  $114\text{ }^\circ\text{C}$ .<sup>44</sup>

In addition to the formation of  $\text{SnI}_x\text{Cl}_y$ , other products and complexes are also evident in the  $^{119}\text{Sn}$  NMR. Here, DHCl shows several additional strong peaks, including at -540, -558, -825, and -845 ppm. The  $^1\text{H}$  NMR of DHCl with  $\text{SnI}_4$  shows a large shift in the hydroxyl protons from a doublet centered at 8.83 ppm to a broad singlet at 6.8 ppm and a reduction in the integrated intensity. This combination of  $^{119}\text{Sn}$  and  $^1\text{H}$  NMR strongly supports that DHCl is forming a coordination complex with the Sn species through the hydroxyl groups, potentially with one of the hydroxyl groups becoming deprotonated. The coordination of Sn species is not unique to DHCl, as all additives investigated with hydroxyl or carboxylic acid groups show significant shifts and broadening of the hydroxyl and carboxylic acid protons upon  $\text{SnI}_4$  addition (SI Figures S14-S17). The ability of these additives to coordinate Sn species in solution is also expected to have an impact on the amount of  $\text{Sn}^{4+}$  in HP films due to reduced reactivity of the coordinated Sn species. Aside from  $\text{BHzHCl}$ ,  $\text{DHCl}$ , and  $\text{HzHCl}$ , the only other additive that shows a large decrease in the amount of  $\text{SnI}_4$  present is  $\text{DHCA}$ . When  $\text{DHCA}$  is added to  $\text{SnI}_4$  new peaks in the  $^{119}\text{Sn}$  NMR spectrum appear at -825 and -1238 ppm, the carboxylic acid proton shifts up field by 2.5 ppm, and the hydroxyl group protons shift down field by 0.5 ppm. These results indicate strong coordination between the Sn complexes and  $\text{DHCA}$ .

Further investigation into solution behavior of Sn species upon addition of various additives was carried out by recording cyclic voltammograms of  $\text{SnI}_2 + \text{FAI} + \text{SnI}_4$  solutions with

and without additives, as displayed in SI Figure S8. When HZHCl, BHZHCl, DHCl, or DHCA are added to the Sn-HP precursor solutions with SnI<sub>4</sub> there is a decrease in the current arising from SnI<sub>4</sub> reduction. (Figure S8A, B). This decrease in current may arise from a combination of the formation of SnI<sub>x</sub>Cl<sub>y</sub> species, as SnCl<sub>4</sub> shows a significantly higher reduction potential than SnI<sub>4</sub> (Figure S8C), and strong coordination between SnI<sub>4</sub> and the additive that shifts the reduction potential of SnI<sub>4</sub>. Absorbance of SnI<sub>4</sub> in solution with HZHCl, BHZHCl and DHCl additives show large (78, 48 and 55%, respectively) decreases in SnI<sub>4</sub> absorbance at 400 nm (Figure S9), which agrees with the decreased SnI<sub>4</sub> concentration observed in CV and NMR. The absorbance of SnI<sub>4</sub> at 400 nm also decreases with DHCA. Although, the decrease is only 33%, suggesting either strong coordination between SnI<sub>4</sub> and DHCA or fractional reduction of SnI<sub>4</sub> to SnI<sub>2</sub>. Based on the <sup>119</sup>Sn NMR, if SnI<sub>2</sub> is formed upon reaction with DHCA, the SnI<sub>2</sub> is coordinated to DHCA.

We now shift to how solution behavior relates to the concentration of Sn<sup>2+</sup> and Sn<sup>4+</sup> in the FASnI<sub>3</sub> films. We initially fabricated Sn-HP films with additive concentrations of 0.5, 1, and 2.5% and recorded the UV-Vis absorbance and photoluminescence (PL) spectra, as displayed in Supporting Information Figures S3 and S4. Nearly all additives show an enhancement in the PL intensity at all additive concentrations. Furthermore, x-ray diffraction spectra (SI Figure S5) are similar for all FASnI<sub>3</sub> films with 2.5% of the additives incorporated. All additives were thus incorporated at 2.5% for the XPS and UPS measurements to increase our ability to detect their effects on the FASnI<sub>3</sub> films. Here, using XPS we probed the concentration of Sn<sup>4+</sup> relative to Sn<sup>2+</sup> for the FASnI<sub>3</sub> films with various additives, as shown in Figure 4 and SI Figure S6. In the control FASnI<sub>3</sub> sample with no additive the Sn<sup>4+</sup> content is 6.9% and Sn<sup>2+</sup> is 93.1%. Similar Sn<sup>4+</sup> concentrations between 6.1 and 7.6% are found with 1,8-DHAQ, NQ, DHBQ, HQ, and 4-FBH. As may be expected, none of these additives show reduction potentials suitable for reducing SnI<sub>4</sub>.

The three HCl containing additives, BHzHCl, HzHCl, and DHCl, all show a depressed concentration of  $\text{Sn}^{4+}$  relative to the control, with  $\text{Sn}^{4+}$  concentrations of 3.6, 4.5, and 5.1%, respectively. DHCA, which diminished the free  $\text{SnI}_4$  concentration based on the  $^{119}\text{Sn}$  NMR also shows a significant decrease in  $\text{Sn}^{4+}$  content at 4.1%.

Surprisingly, DHNT displays the lowest  $\text{Sn}^{4+}$  concentration of 3.3% relative to  $\text{Sn}^{2+}$ . We attribute this low  $\text{Sn}^{4+}$  content with DHNT to two methods of antioxidant behavior, including the reaction of DHNT with oxygen to prevent the reaction of oxygen with the Sn-HP and coordination to Sn species at the perovskite surface. The reaction of DHNT with oxygen is supported by  $^1\text{H}$  NMR measurements (SI Figure S16), where DHNT shows a decrease in the hydroxyl proton intensity and massive broadening of the remaining proton signal following exposure to ambient atmosphere. The same behavior is also observed when  $\text{SnI}_2$  is present with DHNT at a 1:1 mole ratio.

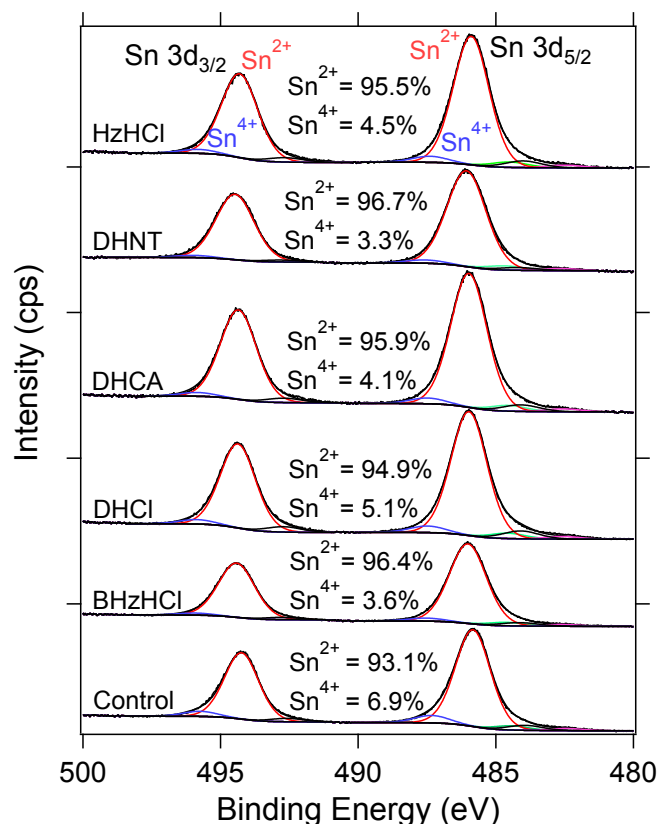


**Figure 4.** XPS spectra of the Sn 3d region for FASnI<sub>3</sub> films with fits to the Sn<sup>2+</sup> and Sn<sup>4+</sup> peaks for the films made with 2.5 mol% of varying additives.

Ultraviolet photoelectron spectroscopy can also provide insight into the concentration of Sn<sup>4+</sup>, as the presence of Sn<sup>4+</sup> leads to high concentrations of holes (*p*-type charge carriers) in FASnI<sub>3</sub>. Here, a more *p*-type film will, to a first approximation, be associated with a higher work function and a valence band onset that is closer to the Fermi energy ( $E_F$ ). The FASnI<sub>3</sub> film without any additive shows a work function of 4.85 eV, which is similar to FASnI<sub>3</sub> with the additives that showed comparable Sn<sup>4+</sup> compositions (Figure 5, SI Figure S7 and Table S2). On the other hand, when the Sn<sup>4+</sup> composition determined by XPS decreases, the work function also generally decreases and the valence band onset shifts further from  $E_F$ . For example, DHNT shows the lowest work function and the lowest Sn<sup>4+</sup> content and BHzHCl, DHCl, and DHCA all have lower Sn<sup>4+</sup> content and work functions that are 0.3 to 0.4 eV lower than the control. These UPS results agree

with the  $\text{Sn}^{4+}$  concentrations determined by XPS and support that increased  $\text{Sn}^{4+}$  content leads to more *p*-type character.

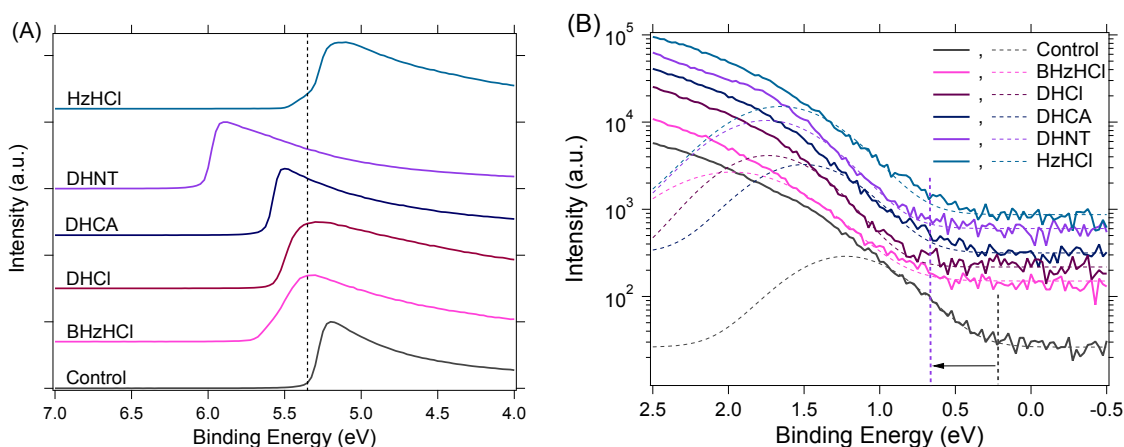


**Figure 5.** UPS spectra of  $\text{FASnI}_3$  film with 2.5 mol% varying additives A) the secondary electron cut-off regions, B) the valence band onset regions.

The various pathways through which the additives can influence the defect states present in Sn halide perovskites are summarized in Figure 6. The ability of the additive to coordinate  $\text{SnI}_2$  and Sn species at grain boundaries and surfaces of  $\text{FASnI}_3$  films is one parameter that can significantly impact the amount of  $\text{SnI}_2$  present. For example, both the  $^{119}\text{Sn}$  and  $^1\text{H}$  NMR support that DHCA coordinates with Sn halide species in solution and reduces the concentration of  $\text{Sn}^{4+}$  in the  $\text{FASnI}_3$  films. Another important consideration is the ability of the additive to reduce  $\text{SnI}_4$  to  $\text{SnI}_2$ , although reduction of  $\text{SnI}_4$  to  $\text{SnI}_2$  does not appear to be a primary mode of action for most organic additives used thus far in Sn-HPs. Identification of additives that can reduce  $\text{SnI}_4$  to  $\text{SnI}_2$  without over reduction to metallic Sn is a promising path forward; however, it may be important that these reducing additives be driven off during thermal annealing to prevent them from acting as charge traps in the Sn-HP films. Halide exchange with both  $\text{SnF}_2$  and chloride containing salts is a clear route for reducing the debilitating impact of  $\text{Sn}^{4+}$  on Sn-PSCs, and our work clarifies that halide exchange occurs with HCl salts that are being applied to improve Sn-PSCs.<sup>28,45,46</sup> Finally,

the additive may act as a sacrificial antioxidant to impede the oxidation of Sn species in the solution or solid state. We propose that it will be necessary to consider multiple of these factors when designing additives, or combinations of additives, for Sn-HPs. For example, two additives with different primary functions may be necessary. In this case one additive could reduce  $\text{SnI}_4$  to  $\text{SnI}_2$  in solution and be driven off during Sn-HP formation, and another additive could coordinate Sn species at surfaces and grain boundaries to prevent oxidation after film formation.

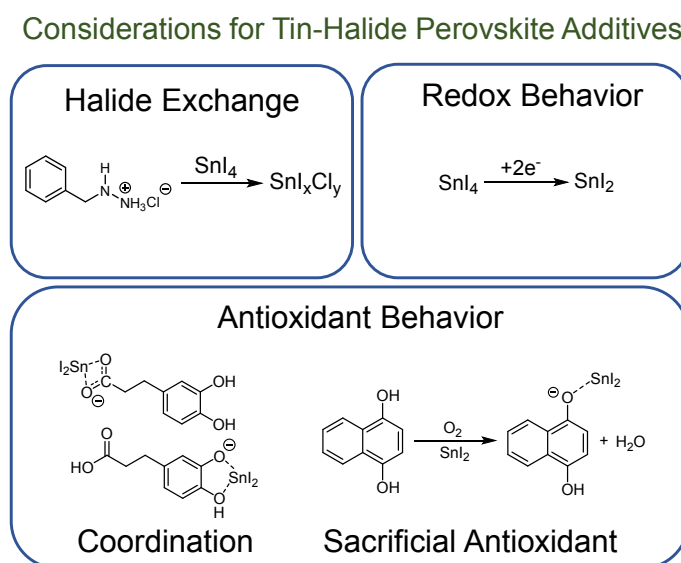


**Figure 6.** Schematic of the various mechanisms through which additives can influence the concentration of  $\text{Sn}^{4+}$  species and their impact on material properties.

### Conclusions:

In summary, the work presented here identifies an ideal range for the reduction potentials of additives to remove  $\text{SnI}_4$  impurities and shows that many commonly used additives do not fall within this ideal range. Identifying and applying reducing agents that can both fully reduce  $\text{SnI}_4$  to  $\text{SnI}_2$  and coordinate Sn at the Sn-HP surface to prevent further Sn oxidation is a promising path forward for improving Sn-based PSCs. We also show that  $\text{SnI}_4$  readily undergoes halide exchange when  $\text{Cl}^-$  is present in solution, likely resulting in less harmful defect states in the Sn-HP film or

evaporation of  $\text{Sn}^{4+}$  species ( $\text{SnI}_x\text{Cl}_y$ ) from the film. This halide exchange may be a primary explanation for the success of several additives for Sn-HPs. Through UPS and XPS we show that the lowest  $\text{Sn}^{4+}$  content is found for an additive that does not reduce  $\text{SnI}_4$  or result in the formation of  $\text{SnI}_x\text{Cl}_y$  complexes. The ability of this additive, DHNT, to lower the concentration of  $\text{Sn}^{4+}$  in  $\text{FASnI}_3$  films is attributed to its reactivity with oxygen as a sacrificial antioxidant and its coordination to Sn. Overall, our work highlights that the reduction potential, coordination with Sn species, ability to react with oxygen, and the potential for halide exchange should all be taken into consideration when evaluating or designing additives for Sn-HPs.

### **Conflicts of Interest**

There are no conflicts of interest to declare.

### **Acknowledgements:**

S.J., K.R.G., and A.J.H. acknowledge support from the National Science Foundation under cooperative agreement No. 1849213. H.R.A., H.P., and K.R.G. acknowledge the U.S. Department of Energy, Office of Science, Basic Energy Sciences under Award Number DE-SC0018208 for supporting the XPS and UPS measurements. A.J.H. acknowledges the University of Kentucky for providing start-up funding. A.F.M. acknowledges the U.S. Department of Energy, Established Program to Support Competitive Research, DE-SC0021283, and the National Science Foundation CHE 2108134 for supporting the NMR measurements.

### **Reference:**

- 1 A. Kojima, K. Teshima, Y. Shirai and T. Miyasaka, *J. Am. Chem. Soc.*, 2009, **131**, 6050–

- 6051.
- 2 J. Jeong, M. Kim, J. Seo, H. Lu, P. Ahlawat, A. Mishra, Y. Yang, M. A. Hope, F. T. Eickemeyer, M. Kim, Y. J. Yoon, I. W. Choi, B. P. Darwich, S. J. Choi, Y. Jo, J. H. Lee, B. Walker, S. M. Zakeeruddin, L. Emsley, U. Rothlisberger, A. Hagfeldt, D. S. Kim, M. Grätzel and J. Y. Kim, *Nature*, 2021, **592**, 381–385.
  - 3 X. Jiang, Z. Zang, Y. Zhou, H. Li, Q. Wei and Z. Ning, *Accounts Mater. Res.*, 2021, **2**, 210–219.
  - 4 X. Jiang, H. Li, Q. Zhou, Q. Wei, M. Wei, L. Jiang, Z. Wang, Z. Peng, F. Wang, Z. Zang, K. Xu, Y. Hou, S. Teale, W. Zhou, R. Si, X. Gao, E. H. Sargent and Z. Ning, *J. Am. Chem. Soc.*, 2021, **143**, 10970–10976.
  - 5 W. Ke and M. G. Kanatzidis, *Nat. Commun.*, 2019, **10**, 965.
  - 6 M. Pitaro, E. K. Tekelenburg, S. Shao and M. A. Loi, *Adv. Mater.*, , DOI:10.1002/adma.202105844.
  - 7 P. J. Smith, *Chemistry of Tin*, Springer Netherlands, 1998.
  - 8 N. K. Noel, S. D. Stranks, A. Abate, C. Wehrenfennig, S. Guarnera, A.-A. Haghighirad, A. Sadhanala, G. E. Eperon, S. K. Pathak, M. B. Johnston, A. Petrozza, L. M. Herz and H. J. Snaith, *Energy Environ. Sci.*, 2014, **7**, 3061.
  - 9 C. C. Stoumpos, C. D. Malliakas and M. G. Kanatzidis, *Inorg. Chem.*, 2013, **52**, 9019–38.

- 10 Z. Chen, J. J. Wang, Y. Ren, C. Yu and K. Shum, *Appl. Phys. Lett.*, 2012, **101**, 093901.
- 11 M. Awais, R. L. Kirsch, V. Yeddu and M. I. Saidaminov, *ACS Mater. Lett.*, 2021, **3**, 299–307.
- 12 L. Lanzetta, T. Webb, N. Zibouche, X. Liang, D. Ding, G. Min, R. J. E. Westbrook, B. Gaggio, T. J. Macdonald, M. S. Islam and S. A. Haque, *Nat. Commun.*, 2021, **12**, 1–11.
- 13 M. Ozaki, Y. Katsuki, J. Liu, T. Handa, R. Nishikubo, S. Yakumaru, Y. Hashikawa, Y. Murata, T. Saito, Y. Shimakawa, Y. Kanemitsu, A. Saeki and A. Wakamiya, *ACS Omega*, 2017, **2**, 7016–7021.
- 14 C. Wang, F. Gu, Z. Zhao, H. Rao, Y. Qiu, Z. Cai, G. Zhan, X. Li, B. Sun, X. Yu, B. Zhao, Z. Liu, Z. Bian and C. Huang, *Adv. Mater.*, 2020, **32**, 1907623.
- 15 Q. Tai, X. Guo, G. Tang, P. You, T. W. Ng, D. Shen, J. Cao, C. K. Liu, N. Wang, Y. Zhu, C. S. Lee and F. Yan, *Angew. Chemie - Int. Ed.*, 2019, **58**, 806–810.
- 16 H. Liu, L. Wang, R. Li, B. Shi, P. Wang, Y. Zhao and X. Zhang, *ACS Energy Lett.*, 2021, **6**, 2907–2916.
- 17 C. M. Tsai, Y. P. Lin, M. K. Pola, S. Narra, E. Jokar, Y. W. Yang and E. W. G. Diau, *ACS Energy Lett.*, 2018, **3**, 2077–2085.
- 18 E. Jokar, C.-H. Chien, C.-M. Tsai, A. Fathi and E. W.-G. Diau, *Adv. Mater.*, 2018, 1804835.

- 19 B.-B. Yu, Z. Chen, Y. Zhu, Y. Wang, B. Han, G. Chen, X. Zhang, Z. Du and Z. He, *Adv. Mater.*, 2021, **33**, 2102055.
- 20 M. Abdel-Shakour, T. H. Chowdhury, K. Matsuishi, I. Bedja, Y. Moritomo and A. Islam, *Sol. RRL*, 2021, **5**, 2000606.
- 21 T.-B. Bin Song, T. Yokoyama, C. C. Stoumpos, J. Logsdon, D. H. Cao, M. R. Wasielewski, S. Aramaki and M. G. Kanatzidis, *J. Am. Chem. Soc.*, 2017, **139**, 836–842.
- 22 T. Wang, Q. Tai, X. Guo, J. Cao, C. K. Liu, N. Wang, D. Shen, Y. Zhu, C. S. Lee and F. Yan, *ACS Energy Lett.*, 2020, **5**, 1741–1749.
- 23 T.-B. Song, T. Yokoyama, J. Logsdon, M. R. Wasielewski, S. Aramaki and M. G. Kanatzidis, *ACS Appl. Energy Mater.*, 2018, **1**, 4221–4226.
- 24 S. Gupta, D. Cahen and G. Hodes, *J. Phys. Chem. C*, 2018, **122**, 13926–13936.
- 25 F. Li, C. Zhang, J. H. Huang, H. Fan, H. Wang, P. Wang, C. Zhan, C. M. Liu, X. Li, L. M. Yang, Y. Song and K. J. Jiang, *Angew. Chemie - Int. Ed.*, 2019, **58**, 6688–6692.
- 26 S. Tsarev, A. G. Boldyreva, S. Y. Luchkin, M. Elshobaki, M. I. Afanasov, K. J. Stevenson and P. A. Troshin, *J. Mater. Chem. A*, 2018, **6**, 21389–21395.
- 27 F. Li, H. Fan, J. Zhang, J. H. Huang, P. Wang, C. Gao, L. M. Yang, Z. Zhu, A. K. Y. Jen, Y. Song and K. J. Jiang, *Sol. RRL*, 2019, **3**, 1900285.
- 28 J. You, M. Wang, C. Xu, Y. Yao, X. Zhao, D. Liu, J. Dong, P. Guo, G. Xu, C. Luo, Y.

- Zhong and Q. Song, *Sustain. Energy Fuels*, 2021, **5**, 2660–2667.
- 29 M. E. Kayesh, T. H. Chowdhury, K. Matsuishi, R. Kaneko, S. Kazaoui, J.-J. Lee, T. Noda and A. Islam, *ACS Energy Lett.*, 2018, **3**, 1584–1589.
- 30 R. Lin, K. Xiao, Z. Qin, Q. Han, C. Zhang, M. Wei, M. I. Saidaminov, Y. Gao, J. Xu, M. Xiao, A. Li, J. Zhu, E. H. Sargent and H. Tan, *Nat. Energy* 2019 410, 2019, **4**, 864–873.
- 31 Q. Chen, J. Luo, R. He, H. Lai, S. Ren, Y. Jiang, Z. Wan, W. Wang, X. Hao, Y. Wang, J. Zhang, I. Constantinou, C. Wang, L. Wu, F. Fu and D. Zhao, *Adv. Energy Mater.*, 2021, **11**, 2101045.
- 32 J. Pascual, M. Flatken, R. Félix, G. Li, S. H. Turren-Cruz, M. H. Aldamasy, C. Hartmann, M. Li, D. Di Girolamo, G. Nasti, E. Hüsam, R. G. Wilks, A. Dallmann, M. Bär, A. Hoell and A. Abate, *Angew. Chemie Int. Ed.*, 2021, **60**, 21583–21591.
- 33 T. Takashima, K. Hashimoto and R. Nakamura, *J. Am. Chem. Soc.*, 2012, **134**, 1519–1527.
- 34 T. Nakamura, S. Yakumaru, M. A. Truong, K. Kim, J. Liu, S. Hu, K. Otsuka, R. Hashimoto, R. Murdey, T. Sasamori, H. Do Kim, H. Ohkita, T. Handa, Y. Kanemitsu and A. Wakamiya, *Nat. Commun.*, 2020, **11**, 1–8.
- 35 W. Li, J. Li, J. Li, J. Fan, Y. Mai and L. Wang, *J. Mater. Chem. A*, 2016, **4**, 17104–17110.
- 36 X. Meng, T. Wu, X. Liu, X. He, T. Noda, Y. Wang, H. Segawa and L. Han, *J. Phys. Chem. Lett.*, 2020, **11**, 2965–2971.

- 37 X. Xu, C.-C. Chueh, Z. Yang, A. Rajagopal, J. Xu, S. B. Jo and A. K.-Y. Jen, *Nano Energy*, 2017, **34**, 392–398.
- 38 X. He, T. Wu, X. Liu, Y. Wang, X. Meng, J. Wu, T. Noda, X. Yang, Y. Moritomo, H. Segawa and L. Han, *J. Mater. Chem. A*, 2020, **8**, 2760–2768.
- 39 M. I. Saidaminov, I. Spanopoulos, J. Abed, W. Ke, J. Wicks, M. G. Kanatzidis and E. H. Sargent, *ACS Energy Lett.*, 2020, **5**, 1153–1155.
- 40 J. Pascual, G. Nasti, M. H. Aldamasy, ac A. Joel Smith, M. Flatken, N. Phung, D. Di Girolamo, S.-H. Turren-Cruz, M. Li, ae André Dallmann, R. Avolio and A. Abate, *Mater. Adv.*, 2020, **1**, 1066–1070.
- 41 M. T. Huynh, C. W. Anson, A. C. Cavell, S. S. Stahl and S. Hammes-Schiffer, *J. Am. Chem. Soc.*, 2016, **138**, 15903–15910.
- 42 B. Wrackmeyer, *Annu. Reports NMR Spectrosc.*, 1985, **16**, 73–186.
- 43 J. J. Burke and P. C. Lauterbur, *J. Am. Chem. Soc.*, 1961, **83**, 326–331.
- 44 D. R. Lide, Ed., *CRC Handbook of Chemistry and Physics. 81st Edition*, CRC Press LLC, Boca Raton, FL, 81st edn., 2000.
- 45 S. J. Yang, J. Choi, S. Song, C. Park and K. Cho, *Sol. Energy Mater. Sol. Cells*, 2021, **227**, 111072.
- 46 J. Zhou, M. Hao, Y. Zhang, X. Ma, J. Dong, F. Lu, J. Wang, N. Wang and Y. Zhou,

*Matter*, 2022, **5**, 683–693.